

Opposing Temperature Dependence of the Stretching Response of Single PEG and PNiPAM Polymers

Aдрианна Колберг,[†] Christiane Wenzel,[†] Klara Hackenstrass,[†] Richard Schwarzl,^{‡,§} Christian Rüttiger,^{§,||} Thorsten Hugel,^{*,†,||} Markus Gallei,^{§,⊥} Roland R. Netz,^{*,‡} and Bizan N. Balzer^{*,†,||}

[†]Institute of Physical Chemistry, Albert-Ludwigs-Universität Freiburg, Albertstraße 23a, 79104 Freiburg, Germany

[‡]Department Institute of Theoretical Bio- and Soft Matter Physics, Freie Universität Berlin, Arnimallee 14, 14195 Berlin, Germany

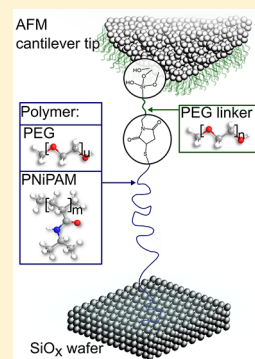
[§]Ernst-Berl-Institute of Technical and Macromolecular Chemistry, Technische Universität Darmstadt, Alarich-Weiss-Straße 4, 64287 Darmstadt, Germany

^{||}Cluster of Excellence livMatS@FIT, Freiburg Center for Interactive Materials and Bioinspired Technologies, University of Freiburg, Georges-Köhler-Allee 105, 79110 Freiburg, Germany

[⊥]Organic Macromolecular Chemistry, Saarland University, Campus Saarbrücken C4 2, 66123 Saarbrücken, Germany

Supporting Information

ABSTRACT: The response of switchable polymer blends and coatings to temperature variation is important for the development of high-performance materials. Although this has been well studied for bulk materials, a proper understanding at the molecular level, in particular for high stretching forces, is still lacking. Here we investigate the molecular details of the temperature-dependent elastic response of two widely used water-soluble polymers, namely, polyethylene glycol (PEG) and poly(*N*-isopropylacrylamide) (PNiPAM) with a combined approach using atomic force microscopy (AFM) based single molecule force spectroscopy (SMFS) experiments and molecular dynamics (MD) simulations. SMFS became possible by the covalent attachment of long and defined single polymers featuring a functional end group. Most interestingly, varying the temperature produces contrasting effects for PEG and PNiPAM. Surprising as these results might occur at first sight, they can be understood with the help of MD simulations in explicit water. We find that hydration is widely underestimated for the mechanics of macromolecules and that a polymer chain has competing energetic and entropic elastic components. We propose to use the temperature dependence to quantify the energetic behavior for high stretching forces. This fundamental understanding of temperature-dependent single polymer stretching response might lead to innovations like fast switchable polymer blends and coatings with polymer chains that act antagonistically.



INTRODUCTION

Polymer coatings, blends, and composites are common in every household and became a part of our everyday life in the past century. They are fundamental for industrial applications due to their unique molding ability, their robustness, and their light weight.^{1–3} Even though we benefit from all their advantages on a daily basis, their behavior is still not completely understood. In particular, their response to external stimuli like force or temperature change is often only understood at a phenomenological level.

The temperature response of polymers is important for both technical applications and the fundamental understanding of polymer physics.^{4–8} Depending on the technical application, polymer properties have to be maintained over a large temperature range (e.g., in cars), or coil to globule transitions are used to obtain stimuli-responsive materials (e.g., for triggered drug release).^{9–11} In polymer physics, temperature is a fundamental parameter. Therefore, the dependence of polymer properties on temperature is a crucial part of the understanding of polymer mechanics.

Atomic force microscopy (AFM) based single molecule force spectroscopy (SMFS) is a versatile tool for investigating temperature-dependent single polymer mechanics in a liquid environment, in particular when combined with molecular dynamics (MD) simulations.^{12–19} Here we focus on two widely used water-soluble polymers with different temperature response, namely, polyethylene glycol (PEG) and poly(*N*-isopropylacrylamide) (PNiPAM).

In bulk experiments PNiPAM in water undergoes a transition from a coil to a globular conformation at its lower critical solution temperature (LCST) of around 305 K.^{20,21} This LCST is close to the temperature at which most physiological processes occur, which makes PNiPAM promising for the development of controlled drug delivery systems.^{22–25} The coil conformation of PNiPAM below the LCST is thought to be stabilized via formation of hydrogen bond bridges between water molecules and the amide side groups.²⁶ The water molecules align around the hydrophobic

Received: April 23, 2019

Published: June 26, 2019

backbone, making the polymer soluble in water and leading to energetic stabilization. At temperatures above the LCST, the entropy of the polymer–water system dominates, which is unfavorable for the exothermic formation of hydrogen bonds. Thus, the bound water molecules are released to increase their entropy and the polymers collapse into a globular state.²⁷ It still remains unclear whether this is a bulk effect or would also be observed for a single polymer chain. The single molecule stretching response at different temperatures has been measured by AFM but with controversial results. Kutnyanszky et al. have found a linear temperature response without any sign of a sharp transition or minimum around the LCST.²⁸ Cui et al. have claimed that the stretching force has a minimum at the LCST.¹⁶ Liang et al. have found a transition of the force–extension profile from wormlike chain behavior to a Rayleigh–Plateau of constant force at the LCST.¹⁷ Furthermore, Zhang et al. have investigated the solvent-dependent single molecule stretching response of PNiPAM, observing thermally induced multisite adsorption above its LCST.¹⁸ The first study was restricted to a small temperature range of 299–313 K, while the other three studies used the nanofishing method for their AFM-based experiments. There, a polymer physisorbed on a surface, e.g., glass or Au(111), is randomly picked up with a cantilever tip. This leads to several problems, namely, that interactions between different polymer chains physisorbed on the substrate cannot be excluded (bulk effects) and that every time a different polymer might be picked. These issues, as discussed later, led us to revisit PNiPAM's temperature behavior.

PEG is a linear macromolecule consisting of $-(\text{CH}_2-\text{CH}_2-\text{O})-$ repeating units. It is used for medical and technological purposes.^{29–32} Unlike most polymers, PEG is generally soluble in water even for a high degree of polymerization.³³ PEG does not exhibit a LCST transition and could be expected to behave like an ideal entropic elastic spring. This has indeed been confirmed in hexadecane, where the force–extension relation of PEG is in accordance with the freely jointed chain model (FJC).^{34,35} However, in water the situation changes and PEG no longer shows the characteristics of an ideal entropic spring at high stretching forces.^{34,19} The reason is found in the structural change from gauche to trans.³⁵ The ratio of monomers in the trans and gauche conformation during stretching and the number of water bridges was extracted from water-explicit MD simulations. Altogether, a dominant solvent-related effect of energy over entropy was suggested at high stretching forces.¹⁹ Again temperature-dependent SMFS experiments should be able to clarify these points.

Here we compare the force response of PEG and PNiPAM at various temperatures in a combined experimental and theoretical study. This allows us to delineate the molecular details of the different temperature responses of PEG and PNiPAM. While PEG becomes softer at higher temperatures, PNiPAM stiffens with increasing temperature. These seemingly contradictory results can be explained in molecular detail with our combined approach. We anticipate that this will help to guide the development of tailored polymeric materials that have to function over a wide force and temperature range.

METHODS

Chemicals. The chemicals used for cleaning of glassware were ammonia solution (Roth, Karlsruhe, Germany, 28.0–30.0%), hydrogen peroxide solution (Sigma-Aldrich, St. Louis, MO, USA, $\geq 30\%$), and ultrapure water (Purelab Chorus 1, Elga LabWater, Celle,

Germany, 18.2 M Ω cm) for preparing RCA solution with a ratio of 1:1:5. For the functionalization process toluene (Fisher Chemicals, Hampton, NH, USA, 99.99%), ethanol (Roth, Karlsruhe, Germany, $\geq 99.9\%$), HEPES buffer (Pan-Reac AppliChem, Darmstadt, Germany, 99.5%, 10 mM, pH = 7, 50 mM NaCl), silane-PEG-mal (NANOCOS, Boston, MA, USA, $M_w = 5$ kDa, $l_{\text{cont}} = 41$ nm), and HEPES buffer (10 mM HEPES, NaCl 50 mM, pH 7) were used. For the synthesis of PNiPAM all solvents and reagents were purchased from Alfa Aesar (Haverhill, MA, USA), Sigma-Aldrich (St. Louis, MO, USA), Fisher Scientific (Hampton, NH, USA), ABCR (Karlsruhe, Germany) and used as received unless otherwise stated. Deuterated solvents were purchased from Sigma-Aldrich. *N*-Isopropylacrylamide (NiPAM) was recrystallized out of toluene and *n*-hexane (1:1) and dried in vacuum. $\text{Cu}^{(I)}\text{Br}$ was washed five times with glacial acetic acid and ethanol. Tris[2-(dimethylamino)ethyl]amine (Me_6TREN), *N,N*-dimethylformamide (DMF), 2-bromoisobutyric *tert*-butyl ester (*t*BbIB) were stored under argon atmosphere.

Polymers. The polymer used for the PEG experiments was purchased as thiol-PEG-thiol (HS-PEG-SH, Creative PEGWorks, NC, USA, $M_w = 35$ kDa). The expected mean contour length for the experiments was calculated to 282 nm with a monomer length of 0.356 nm and a molecular weight of 44.05 Da.^{35,19} Adding the silane-PEG-mal linker length with about 41 nm leads to a total length of 323 nm.

PNiPAM was synthesized as follows. The corresponding reaction path can be found in Figure S1a: 9.00 g (79.53 mmol) of NiPAM and 3.20 μL (0.018 mmol) of *t*BbIB were placed in a Schlenk tube, and an amount of 18 mL of a 50:50 mixture of ultrapure water and DMF was added. The mixture was degassed twice, and the polymerization was started by adding 90 μL (0.018 mmol) of a 0.2 M solution of $\text{Cu}^{\text{I}}(\text{Me}_6\text{TREN})\text{Br}$ in DMF. After 40 min an amount of 12 mg (0.075 mmol) of potassium ethyl xanthogenate was added. After 10 min the reaction was cooled in an ice bath for 30 min. The mixture was diluted with 160 mL of THF and filtered through an aluminum column to remove the residual copper catalyst. The polymer was precipitated in 800 mL diethyl ether and dried in vacuum (yield, 4.06 g; M_w , 497 kDa; $D = 1.28$).

An amount of 500 mg (0.001 mmol) of the CTA-end-capped PNiPAM was dissolved in 20 mL of ultrapure water, and an amount of 100 mg (2.64 mmol) of NaBH_4 was added. After 2 h the polymer/solvent mixture was dialyzed against water for 4 days. The polymer was obtained by lyophilization (452 mg). An amount of 300 mg of the polymer was dissolved in 10 mL of DMF, and an amount of 45 mg (0.16 mmol) of tris(2-carboxyethyl)phosphine hydrochloride (TCEP) was added. After 24 h the mixture was diluted with water and dialyzed against water for 4 days again. An amount of 243 mg of the resulting polymer was obtained after lyophilization ($M_n = 510$ kDa, $D = 1.28$; see Figure S1b).

For PNiPAM, the monomer length was calculated with respect to the backbone using a C–C bond length of 154 pm and a bond angle of 109.5°. With a calculated monomer length of around 252 pm and a monomer weight of 113 Da, the average contour length could be calculated to 1.14 μm with 4513 repeating units. Adding the silane-PEG-mal linker length with about 41 nm leads to a total length of 1.18 μm .

Polymer Characterization. Standard size-exclusion chromatography (SEC) was performed with a system composed of a 1260 IsoPump G1310B (Agilent Technologies, Santa Clara, CA, USA), a 1260 VV detector G1314F at 254 nm (Agilent Technologies), and a 1260 RI detector G1362A at 35 °C (Agilent Technologies), DMF (with LiCl, 1 g/L) as the mobile phase (flow rate 1 mL/min) on a GRAM column set for DMF (at 50 °C) from PSS (Polymer Standard Service (PSS), Mainz, Germany) (GRAM 30, GRAM 1000, GRAM 1000). Calibration was carried out using PMMA standards for DMF (from PSS). Samples were measured with concentrations between 1 and 3 mg/mL. For data acquisition and evaluation of the measurements, PSS WinGPC UniChrom 8.2 was used.

NMR spectra were recorded on a Bruker DRX 500 spectrometer (Billerica, MA, USA) working at 500 MHz. NMR chemical shifts were referenced relative to the used solvent (D_2O). For data acquisition

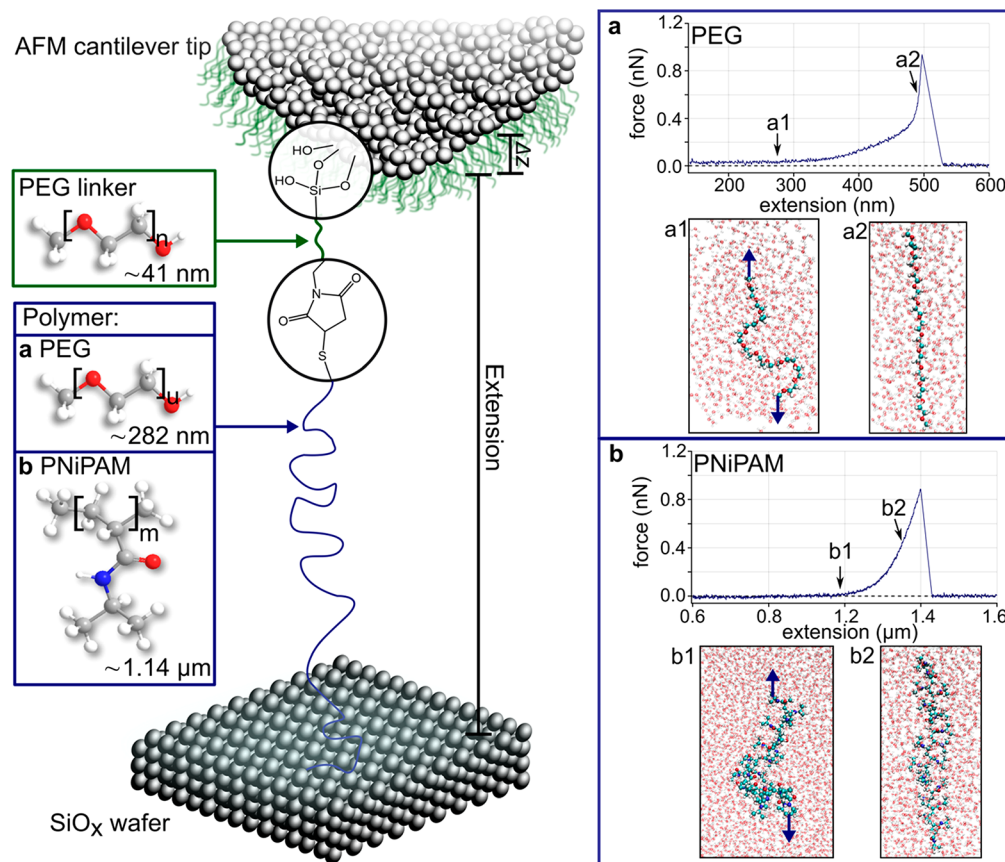


Figure 1. Scheme of an AFM single molecule setup with a zoom-in to the functional groups (circular frames) and an exemplary monomeric unit for the PEG linker (green box) and the polymer (blue box) at room temperature. On the right examples of force–extension curves at 298 K are shown for (a) PEG and (b) PNIPAM including snapshots of the MD simulations at the forces indicated in the force–extension traces. These forces are 15 pN and 600 pN for PEG (a1, a2) and 20 pN and 500 pN for isotactic PNIPAM (b1, b2). The expected monomer numbers in the experiments are $n = 114$ (41 nm) for the PEG linker, $u = 795$ (282 nm) for the PEG, and $m = 4513$ (1.14 μm) for the PNIPAM polymer. Δz indicates a possible vertical shift corresponding to the anchoring position of the polymer on the cantilever tip.

and evaluation of the measurements, NMR software MestReNova 11.0 was used.

Simulation Details. All molecular dynamics simulations are performed with the GROMACS simulation package (version 4.6.5 or newer).³⁷ The time step is set to 2 fs. The temperature is set to a fixed value for each individual simulation. For temperature and pressure coupling, the v-rescale and Parinello–Rahman algorithms are used.^{38,39} The pressure is isotropic and set to 1 bar with a water compressibility of $4.5 \times 10^{-5} \text{ bar}^{-1}$. All simulations are performed with periodic boundary conditions in all three directions. The cutoff of nonbonded interactions is set to 1.0 nm. The particle mesh Ewald method is used for the long-range electrostatic interactions.⁴⁰

For PEG the force field charmm35r is used.⁴¹ The elongated ($\text{H}-[\text{CH}_2-\text{O}-\text{CH}_2]_{12}-\text{H}$) chain is placed in a $3 \text{ nm} \times 3 \text{ nm} \times 9.6 \text{ nm}$ box with 2900 tip3p water molecules. To equilibrate the system, the initial energy minimization of the system is followed by a 10 ps NVT simulation with constant volume and without pressure coupling and a 2 ns NPT simulation with an isotropic pressure of 1 bar. For the production run, the first and the last oxygen atoms are defined as pulling groups. A constant force between 1 pN and 600 pN is applied in the z direction. For low forces, we additionally performed simulations using a longer chain ($\text{H}-[\text{CH}_2-\text{O}-\text{CH}_2]_{24}-\text{H}$) placed in a $4.5 \text{ nm} \times 4.5 \text{ nm} \times 20 \text{ nm}$ box with 13 433 water molecules. Each pulling simulation is performed for at least 200 ns. The temperature remains unchanged throughout a single simulation run and is set to 250, 300, 325, 350, and 400 K, respectively.

For simulations of PNIPAM, parameters remain the same as for PEG if not stated otherwise. For PNIPAM we use a recently modified version of the OPLS-AA force field with partial charges optimized by

comparison to quantum mechanical simulations together with the SPC/E water model.^{42–45} The first and the last C atom of the backbone of $\text{H}-[\text{C}_6\text{H}_{11}\text{NO}]_{20}-\text{H}$, which are adjacent to the side chain of the polymer, are defined as pulling groups. A constant force between 1 pN and 500 pN is applied in the z direction. We simulate isotactic (meso-diad) PNIPAM, where the side chains are located on one side of the backbone, and syndiotactic (racemo-diad) PNIPAM, where the side chains are on alternating sides of the chain. The elongated chain is placed in a $3 \text{ nm} \times 3 \text{ nm} \times 11 \text{ nm}$ box with 3121 SPC/E water molecules. Each pulling simulation is performed for at least 1000 ns. The temperature remains unchanged throughout a single simulation run and is set to 288, 298, 308, and 318 K, respectively.

For both PNIPAM and PEG, the extension in the pull direction is calculated as the time average of the separation in the z direction of the two pulling groups over the course of a simulation. The extension of PEG is normalized by the contour length $L_{C,0} = 11 \times 0.356 \text{ nm}$ or $L_{C,0} = 23 \times 0.356 \text{ nm}$, depending on the polymer length and in accordance to Liese et al.¹⁹ For isotactic PNIPAM the contour length used for normalization is $L_{C,0} = 19 \times 0.266 \text{ nm}$ and for syndiotactic PNIPAM $L_{C,0} = 19 \times 0.264 \text{ nm}$ in accordance to Kanduć et al.⁴⁴

AFM Cantilever Tip Functionalization. The covalent attachment of one single polymer to a cantilever tip is decisive for single molecule force experiments. It enables a high reproducibility when performing force spectroscopy with a certain polymer on a specific cantilever tip. Influences on the measurements like differences in the contour length due to different attachment points to the cantilever tip, variation of the spring constant of the cantilever, or interactions with further polymers can be widely prevented.⁴⁶ Furthermore, a high yield

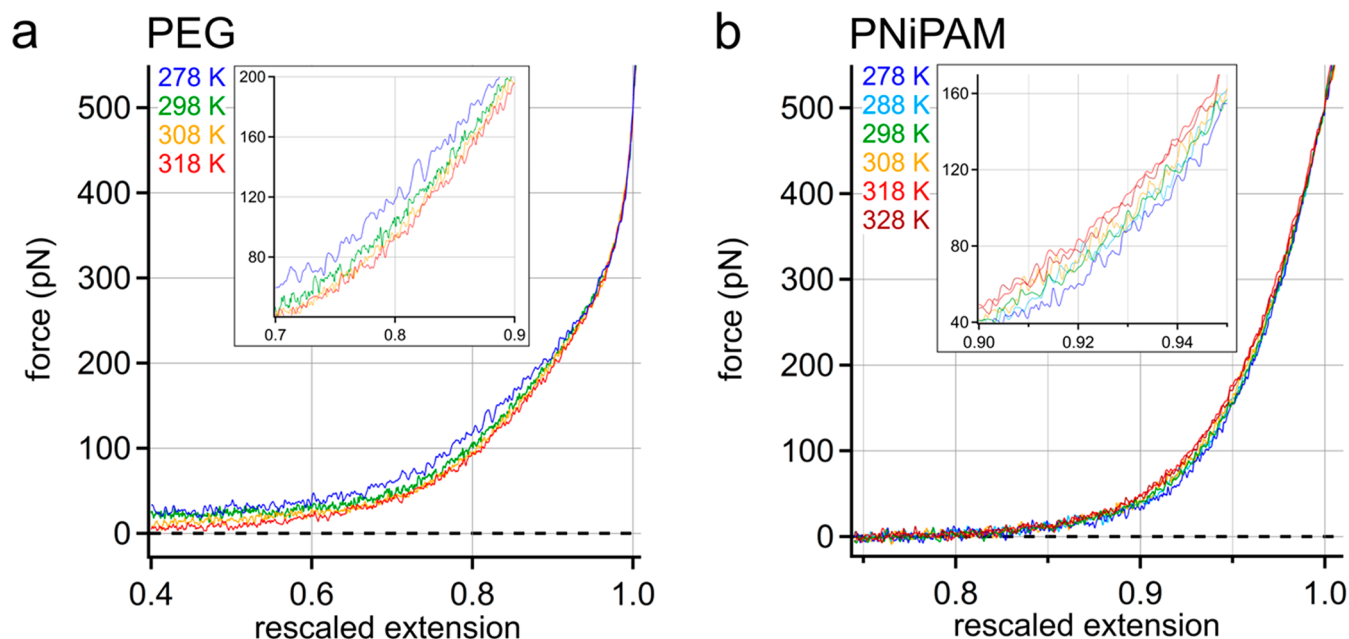


Figure 2. Experimental AFM data: (a) master curves of PEG showing a decreasing stretching force with increasing temperature; (b) master curves of PNiPAM showing an opposite temperature dependence compared to PEG. A single master curve for every temperature was determined based on force–extension curves comprising a stretching event to at least 500 pN. After rescaling of the extensions to the length L_0 at a force of 500 pN, the force–extension curves were averaged by a binomial smoothing.

of single molecule events can be obtained (19% for PEG and 42% for PNiPAM).

Silicon nitride AFM cantilevers, namely, MLCT and MLCT-BIO-DC (both: Bruker AFM probes, Camarillo, CA, USA) were used for all measurements. First, the cantilevers were activated with oxygen plasma to gain hydroxyl groups on the surface of the cantilever tips. While the MLCT probes were treated for 1 min with 20% power, the thermally more stable MLCT-BIO-DC probes were treated for 2 min with 40% power, both at a pressure of 0.1 mbar. As a next step, a 5 kDa silane-PEG-mal (NANOCS, Boston, MA, USA) linker was bound to the cantilever tip. The linker enabled us to couple a probe molecule to the cantilever tip via a covalent bond. Therefore, the cantilevers were incubated in a solution of silane-PEG-mal in toluene (1.25 mg/mL, 3 h, 60 °C).⁴⁷ Even though the cantilever tip is covered with maleimide groups, these undergo a hydrolysis in water (inactive PEGs) leaving just few binding sites for the single probe polymer to be attached.⁴⁸ The inactive PEGs serve as a passivation layer to reduce undesirable interaction between the cantilever tip and an underlying surface as well as between the single PEG polymer and the cantilever tip. For functionalization with PEG, the PEGylated cantilevers were rinsed in toluene and incubated in a solution of SH-PEG-SH in toluene (1.25 μ g/mL, 1 h, 60 °C). For functionalization with PNiPAM, the PEGylated cantilevers were rinsed in toluene and ethanol before incubation in a solution of PNiPAM-SH in ethanol (1.25 μ g/mL, 3 h, room temperature). After a final rinsing, the cantilevers were stored in HEPES buffer at 4 °C until use in the AFM experiment.

For every functionalization, control cantilevers were additionally prepared by the same procedure incubating the cantilevers in the pure solvent instead of the SH-PEG-SH or the PNiPAM-SH solution. A scheme of an AFM-based single molecule force spectroscopy setup can be found in Figure 1.

AFM Measurements. All measurements were performed with a Cypher ES (Asylum Research, an Oxford Instruments company, Santa Barbara, CA, USA) using a heating and cooling sample stage for temperature variation. All measurements took place in ultrapure water on a silicon oxide wafer cleaned in ethanol using a sonicator (Elmasonic S15, Elma, Singen, Germany). Before every measurement, the inverse optical lever sensitivity (InvOLS) was determined by fitting a linear function to the repulsive regime of a force–extension

curve. In order to reduce errors, the determination of the InvOLS was performed by using an average of at least five individual InvOLS values. The spring constant of the cantilever was determined by the thermal noise method.⁴⁹

The measurement parameters were defined as follows: force distance, 1–3 μ m; velocity, 1 μ m/s; trigger point, 500 pN; sampling rate, 5 kHz; dwell time toward the surface, 0–1 s. To minimize the influence of the probe, force–extension curves were recorded in a gridlike manner with 10×10 points covering $20 \times 20 \mu\text{m}^2$ (force maps). At least two force maps were obtained per cantilever, with and without dwell. The temperature was varied in a random order. Following a temperature change, force–extension curves were collected after a stabilization time of at least 5 min. Prior to a series of measurements, at least one control cantilever was measured on different spots to ensure the cleanliness of the SiO_x surface and a contamination-free functionalization. Once the control cantilevers showed an absence of stretching events, the PEG or PNiPAM functionalized cantilevers were measured, respectively.

For data evaluation, a self-programmed evaluation software based on Igor Pro (Wavemetrics, Portland, OR, USA) was used. The force–extension curves were corrected for drift by fitting a linear function to the baseline after the last stretch. Then, the linear function was subtracted from the force–extension curve leading to curves such as shown in Figure 1a and Figure 1b.

Even though we used PNiPAM polymers with a low polydispersity index value $\mathcal{D} = 1.28$, significant differences in the polymer lengths were observed in the AFM experiments. This observation can be explained by different phenomena, which have already been described in literature before.¹⁹ The common method to detect the molecular weight and the polydispersity is size-exclusion chromatography (SEC), which determines a relative weight of the polymer compared to standards like polystyrene or poly(methyl methacrylate).⁵⁰ As polymers can significantly differ with respect to their hydrodynamic volume compared to these standards, a deviation of the determined molecular weight of PNiPAM from the absolute molecular weight is expected. Another important influence is given by the silan layer. During the functionalization process in toluene spurious water might start an oligomerization of the silane molecules prior to the attachment to the cantilever tip. This leads to a flexible silane network with fewer anchor points.⁵¹ Furthermore, the anchoring

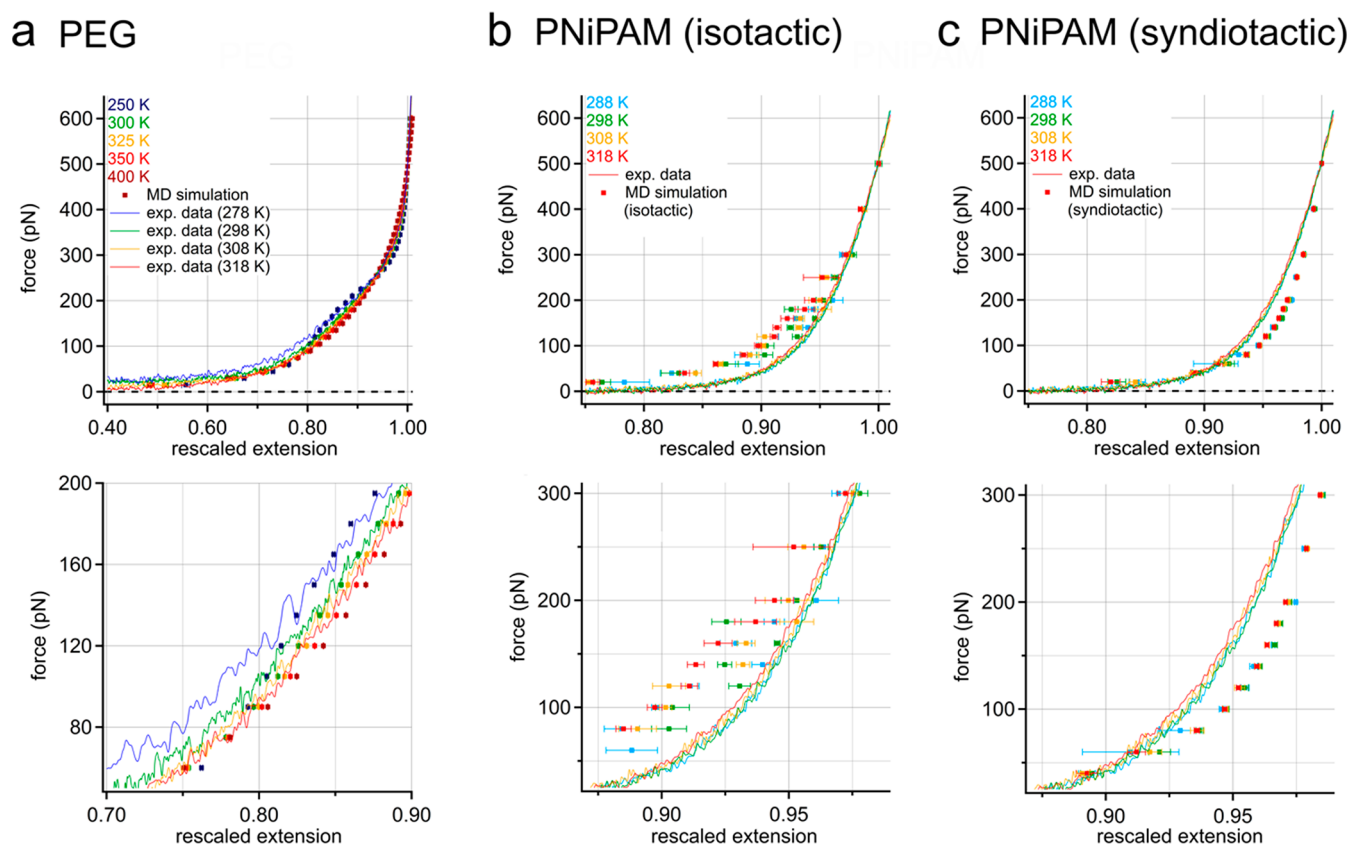


Figure 3. Comparison of MD simulations (circles) with the experimental data (lines): (a) MD simulations for a PEG molecule for a wide temperature range showing the same characteristics as the experimental data. Note the significantly larger temperature range in the simulations. (b) MD simulations of an isotactic and (c) of a syndiotactic PNiPAM polymer compared to the experimental data for atactic PNiPAM, respectively. The experimental force–extension traces are situated between the MD simulations of the syndiotactic and isotactic PNiPAM. Also, the magnitude of the temperature-induced force shift is between the two extreme cases considered in the MD simulations. Respective zoom-ins are shown in the bottom row for better comparison of the relevant mid-force range.

point of the polymer to the cantilever tip might not necessarily be at the apex.¹⁹ As the cantilever detects only a force component in vertical direction, a nonvertical orientation of the polymer between a pinpoint on the substrate and the cantilever tip might lead to a shift of the detected force according to Serr et al.⁵² Yet for long polymers such as the PEG and PNiPAM polymers presented here, the deviation from a vertical orientation is expected to be less than 1°, leading to a force variation below the detection limit of the AFM.⁵³ For PEG, a broad mass distribution is expected (PDI is not indicated by the manufacturer). Furthermore, for HS-PEG-SH it is chemically possible that the ends of two polymers oxidize and react with each other to give a disulfide bridge.⁵⁴ That might lead to length values that are multiples of the contour length. Even though these phenomena have an influence on the observed absolute contour length of the polymer, they do not affect the stretching response of the respective polymer itself. Therefore, all these effects are not expected to show any dependence on temperature and should not affect the general results found here.

RESULTS AND DISCUSSION

Figure 1 shows a schematic of the AFM-based single molecule force experiments including example traces and simulation snapshots. A single stretching event at a contour length of about 350 nm such as given in Figure 1a was observed in the PEG data in 95 of the 500 measured force–extension curves (fraction of 19%). For PNiPAM, 252 out of 600 force–extension curves (42%) were found, such as shown in Figure 1b. In order to discuss the temperature dependence of the force–extension traces, a single master curve for every

temperature was determined using only those curves that show a stretching event to at least 500 pN (see Figures S2 and S5). Then, the extensions were rescaled to a length L_0 at a force of 500 pN where conformational fluctuations and solvent effects are negligible.⁶⁸ Finally, the force–extension curves were averaged by a binomial smoothing, where a Gaussian filter convolves the data with normalized coefficients derived from Pascal's triangle at a level equal to the smoothing parameter 20.⁵⁵ These rescaled traces are shown in Figure 2.

For the PEG master curves depicted in Figure 2a we used 19 traces (4%) in total that reached forces of at least 500 pN in order to investigate the polymer behavior at intermediate and high stretching forces. We focus on the extension range from 0.4 to 1.0 L_0 because the temperature effect is best identified here. Furthermore, we can be sure that this extension range only comprises the stretching of a single molecule (for raw data see Figure S2). The difference between the force–extension curves for PEG measured at different temperatures (Figures 2a and S3) can be described as a decrease of the force with increasing temperature at a given rescaled extension, which is discussed in detail below. In other words, an increase of approximately 5% of rescaled extension (at an applied force of 100 pN) is observed when increasing the temperature from 278 to 318 K. Note that it is crucial to compare the temperature dependence for data taken with one and the same cantilever and for one identical set of polymers. Otherwise, variations of the spring constant of different cantilevers and

possibly the contour length of polymers could mask the temperature effects (see [Methods](#) section for details). A second data set confirms the observed temperature response ([Figure S4](#)).

For PNiPAM, the contour length varies significantly even for a single cantilever tip. In order to minimize the effects of contour length, we selected only traces with contour lengths between 1.0 and 2.5 μm and detachment forces of more than 500 pN. This resulted in 20 traces (3%), which are shown in the master curves depicted in [Figure 2b](#). The raw data can be found in [Figure S5](#). Additionally, [Figure S6](#) shows all master curves for different temperatures. Again, a temperature-dependent shift in the stretching force can be observed but this time in the opposite direction compared to PEG. The stretching forces increase with increasing temperature, i.e., the chain becomes stiffer, for a given rescaled extension (see [Figures S6 and S7](#)). In other words, a decrease of approximately 1% of rescaled extension (at an applied force of 100 pN) is observed when the temperature is increased from 278 to 328 K. It is noteworthy that there is no sudden change in the shape or frequency of the recorded force–extension curves when comparing temperatures below and above the LCST. This agrees with the expectation that a highly stretched single molecule does not show cooperative effects, which would rather be expected for weakly stretched chains that can self-interact.

This is in contrast to the study by Cui et al., which claimed that the stretching force has a minimum at the LCST when examining the temperature range of 304–313 K with a difference of relative extension of up to 10% at 200 pN.¹⁶ Furthermore, we did not observe any plateaus in our force–extension curves over the whole range of temperature values from 278 to 328 K such as observed by Liang et al.¹⁷ Yet both Cui et al. and Liang et al. performed nanofishing experiments. Zhang et al. have already pointed out that cantilever tip functionalization might be a better way to obtain clean and real single molecule stretching events.¹⁸ Nanofishing might lead to cooperative effects that strongly affect the outcome of a single molecule study due to additional substrate-adsorbed molecules.⁵⁶ The covalent attachment of a single molecule to the cantilever tip as presented here enables us to exclude any interactions with neighboring polymers. Therefore, our results are consistent with the study by Kutnyanszky et al.,²⁸ in which single molecule attachment to a cantilever tip had also been carried out. Yet our significantly larger force and temperature ranges allow us to deduce the molecular mechanism for this behavior. A second data set for PNiPAM taken with a different cantilever confirms the observed temperature dependence ([Figure S7](#)). To deepen our understanding of these observations, MD simulations were performed and compared to the experimental data.

[Figure 3a](#) shows a comparison between the experimental master curves and the MD simulations for PEG. The distinct tripartite structure with a middle section exhibiting an almost constant force–extension slope is well reproduced by the simulations. Also, the temperature shift agrees well with the experimental data. This validation enables us to extract the molecular mechanisms for PEG from the MD simulations (see below).

[Figure 3b](#) and [Figure 3c](#) show the comparison of the experimental master curves for PNiPAM with two sets of MD simulations. As the polymer was synthesized by a controlled radical polymerization without any manipulation of the

propagating chain ends, a predominantly atactic arrangement of the side groups is expected. This is confirmed by the ¹³C NMR data, which show the expected ratios between the signals in the range of 30–45 ppm ([Figure S1c](#)).⁵⁷ Accordingly, the experimental force–extension curves are situated between force–extension curves from MD simulations representing the extreme cases of a fully isotactic and a fully syndiotactic polymer, as shown in [Figure 3b](#) (isotactic) and [Figure 3c](#) (syndiotactic). For the isotactic simulations, an extremely slow relaxation of the PNiPAM chain leads to a strong variation of the stretching force, masking any clear trend with respect to temperature. By contrast, the syndiotactic simulations exhibit small error values and present a clear force–extension course for the different temperatures. In particular, the temperature shift in the force response shows the same qualitative behavior for both AFM experiment and MD simulation, although differing quantitatively. The quantitative difference presumably results from the difference between atactic (experiment) and syndiotactic (MD simulation) arrangements.

The temperature dependence of the free energy per length F/L_0 can generally be approximated as T^n with an exponent n . An ideal entropic behavior is predicted by the FJC model,⁵⁸

$$\frac{z_{ete}}{L_c} = \coth \frac{fb}{k_B T} - \frac{k_B T}{fb} \quad (1)$$

while the wormlike chain (WLC) model is not purely entropic,⁵⁹

$$f = \frac{k_B T}{l_p} \left[\frac{z_{ete}}{L_c} + \frac{1}{4 \left(1 - \frac{z_{ete}}{L_c}\right)^2} - \frac{1}{4} \right] \quad (2)$$

Here z_{ete} is the rescaled end-to-end distance, L_c the contour length, b the temperature independent Kuhn length (see [Table S1](#)), and f the applied force. The persistence length is given by $l_p = \kappa/(k_B T)$, where the bending rigidity κ is assumed to be temperature independent. Next, the free energy F is given by

$$F = U - TS \quad (3)$$

While the FJC model leads to $U/F = 0$ and $-TS/F = 1$, the WLC model leads to $U/F = -1$ and $-TS/F = 2$ with the energy U and the entropy S .¹⁹ While in both cases TS/F is constant, F is proportional to T^n with $n = 1$ for the FJC model (for a temperature independent Kuhn length, see [Table S1](#)) and $n = 2$ for the WLC model (for a temperature independent bending rigidity κ). By contrast, a purely energetic stretching response should be temperature independent, i.e., $n = 0$. We name regimes with exponents $n > 1$ as superentropic, $n < 0$ as superenergetic, and with $0 < n < 1$ as mixed.

The commonly used FJC and WLC models fail to describe the force–extension behavior of both PEG and PNiPAM over the whole force range ([Figures S8 and S9](#)).¹⁹ In particular, both polymers deviate from a purely entropic spring model at intermediate and highly stretched states. In fact, they represent superenergetic or mixed springs with different temperature behavior, as discussed below.

The temperature-dependent force response of the PEG polymer is best analyzed by normalization with respect to T^n in order to find the optimal exponent n . The optimal value for n is obtained when the normalized free energy–force curves for the different temperatures superimpose. In particular, the optimal exponent n is found by the lowest coefficient of variation (ratio

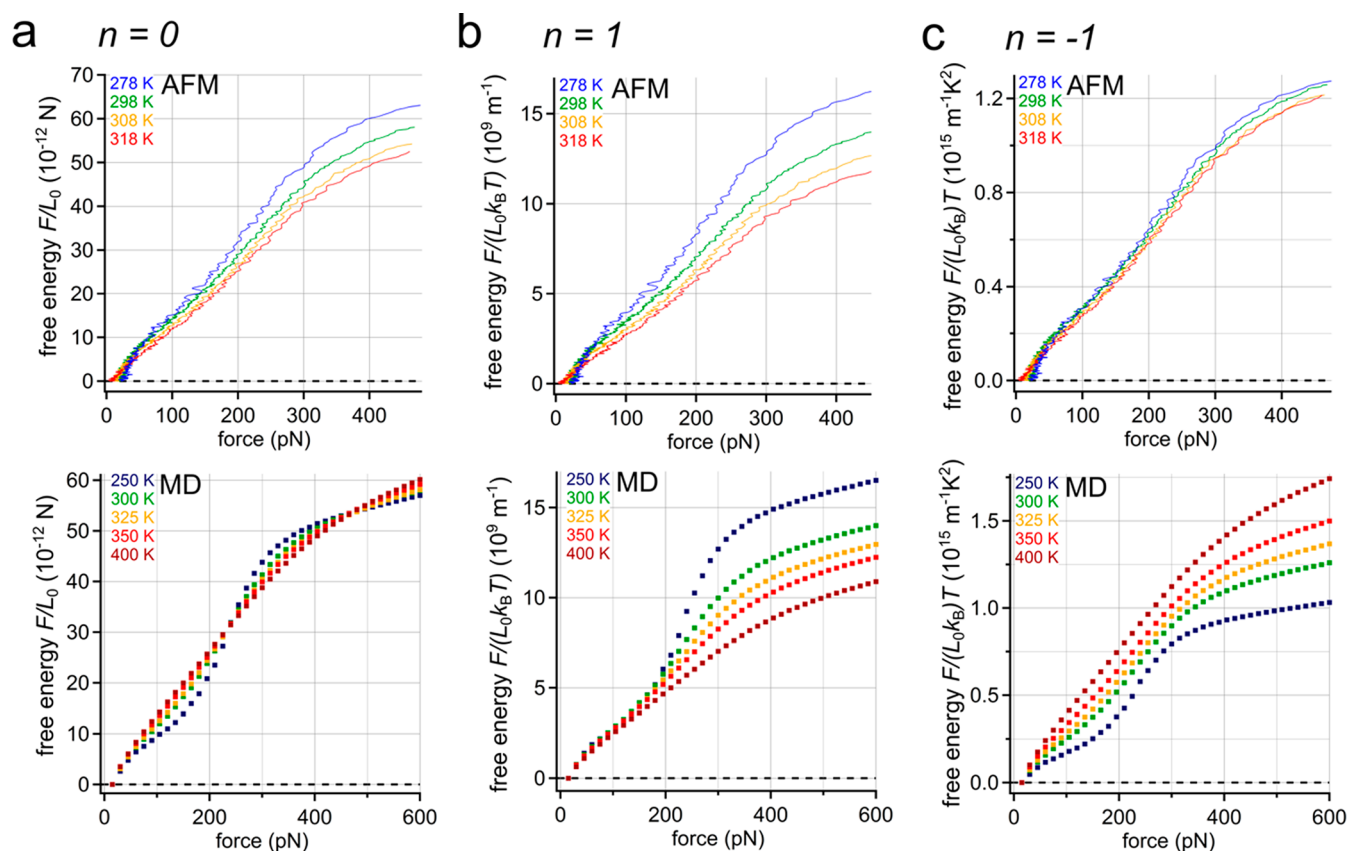


Figure 4. Temperature dependence of the stretching free energy F for experimental AFM data and the MD simulations of PEG: (a) stretching free energy F per L_0 (extension at a force of 500 pN) vs force (case $n = 0$); (b) F per L_0 divided by $k_B T$ ($n = 1$); (c) F per L_0 divided by $k_B T^{-1}$ ($n = -1$). Note the significantly larger temperature range in the simulations.

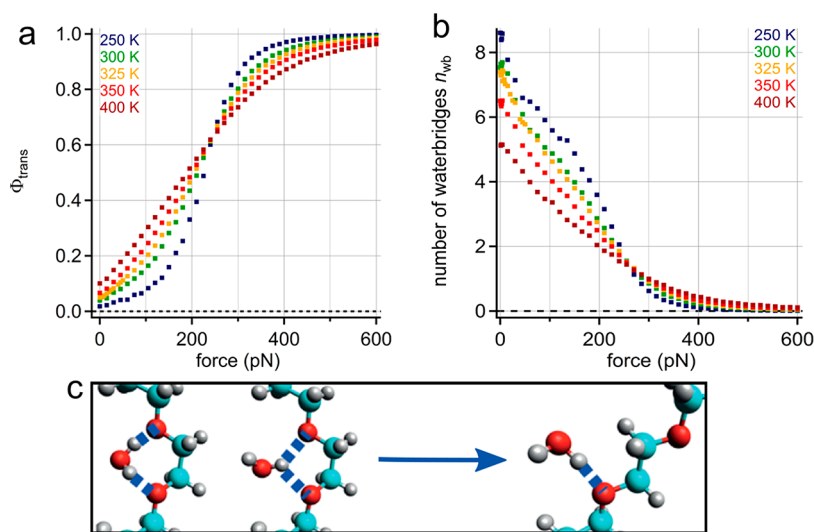


Figure 5. Molecular mechanism of PEG revealed by MD simulation data: (a) mean fraction of monomers in the trans state and (b) number of water bridges n_{wb} vs the stretching force for PEG at different temperatures ranging from 250 to 400 K (with a PEG chain comprising 11 monomers). (c) Schematic picture of PEG in the gauche state with two hydrogen bonds (water bridge) involved (left) and a water molecule forming a single hydrogen bond with PEG in the trans state (right).¹⁹

of standard deviation and mean value) for the different temperatures at each stretching force value (Figure S10). Thus, the different regimes (entropic and energetic) can be distinguished along the course of the stretching force.

In Figure 4 the stretching free energy per length F/L_0 , rescaled with various scaling exponents n , is shown in order to

compare the regimes obtained from experiment and simulation. F is determined by integration of the master curves (force vs rescaled extension) given in Figures 2 and 3. Considering the different temperature ranges for the experiment and the MD simulation, the data agree qualitatively well. For low forces below 150 pN, the MD simulation data are best

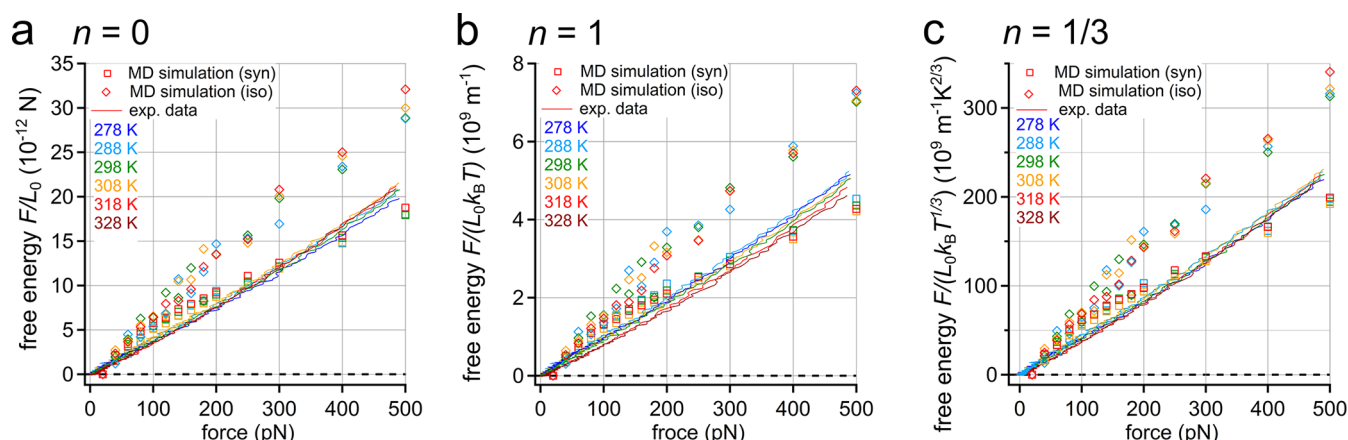


Figure 6. Temperature dependence of the stretching free energy F for the MD simulations of isotactic PNiPAM (open diamonds) and syndiotactic PNiPAM (open squares) compared to experimental AFM data (atactic, lines): (a) stretching free energy F per L_0 (extension at a force of 500 pN) vs force ($n = 0$); (b) F per L_0 divided by $k_B T$ ($n = 1$); (c) F per L_0 divided by $k_B T^{1/3}$ ($n = 1/3$).

described by a scaling exponent $n = 1$, indicating purely entropic behavior (Figure 4b). In the AFM experiments, this purely entropic regime is already left at forces below 100 pN. Then, above 150 pN, more and more energy-dominated behavior is found for both the MD simulations and the AFM experiments. The AFM experiments even reach the super-energetic regime with $n = -1$ (Figure 4c). The MD simulation for the lowest temperature (250 K) shows a nonlinear course, but this temperature cannot be probed in experiments. At higher temperatures (300 K, 325 K, 350 K), where experiment and simulation can directly be compared, the shape of the curves qualitatively agrees well.

Altogether, the MD simulations are best described by an entropy dominated chain ($n = 1$) for forces up to 150 pN and an energetic chain ($n = 0$) starting at this intermediate force. The experiments already show significant superenergetic behavior starting from below 100 pN and finally dominant energetic contributions ($n = -1$) at higher stretching forces.

In order to understand the shift from entropic to energetic behavior, we examined the mean fraction of gauche and trans states in the PEG chain according to MD simulations. Figure 5a shows the mean fraction of monomers in the trans state for different temperatures as a function of force. The initially shallower increase of Φ_{trans} for low temperatures can be explained by a higher number of water bridges forming two hydrogen bonds with the PEG backbone, as depicted in Figure 5b. The decrease in the number of water bridges explains the overall decrease in F/L_0 with increasing temperature (Figure 4a). In addition, the pronounced nonlinear behavior of Φ_{trans} for low temperatures around 250 pN can explain the increase in the slope of F/L_0 observed in Figure 4a at this force. Here the water bridges stabilize the gauche state, which has a smaller contour length compared to the trans state. This also explains the temperature-dependent crossover of PEG around 250 pN, which can be observed in Figures 4a and 5. Note that a temperature-dependent contour length can be obtained using the FJC model to fit PEG force–extension curves (see Figure S8) if a temperature independent Kuhn length is assumed (see Table S1). Such a temperature-dependent contour length would just be a fit parameter with no real physical meaning, and we therefore argue that the exponent n discussed above better describes the underlying physical processes.

Figure 6 shows the stretching free energy for PNiPAM vs force for different temperatures determined analogously to the PEG data. In general, AFM experiments and MD simulations agree well. Again, we optimize the coefficient of variation to find the exponent n in the temperature dependence (Figure S11). For the syndiotactic MD simulations, a dominance of entropy ($n = 1$) up to 100 pN can be observed (Figure 6b). But for higher forces, $n = 1/3$ describes well the course of the temperature dependence of F/L_0 , resulting in a dominance of the energetic character. In fact, the syndiotactic MD simulations are quite close to the atactic experimental data. Altogether, we obtain the best fit for $n = 1/3$, i.e. $F/L_0 \sim T^{1/3}$ (Figure 6c). In general, PNiPAM shows a mixed behavior ($0 < n < 1$) for the investigated stretching forces.

At the molecular scale the temperature-dependent stretching response of PNiPAM can be understood as follows:^{26,60–63} At low temperatures, hydrogen bond bridges are formed between water molecules and the amide side groups. Thus, the polymer comprising a hydrophobic backbone is made soluble in water. When the temperature is increased, exothermic formation of hydrogen bonds becomes unfavorable. Therefore, the bound water molecules are released leading to a partial dehydration of the polymer. In parallel, intramolecular hydrogen bonding between the amide groups is favored (attractive interaction). Therefore, the polymer tends to collapse into a globular state, i.e., more force is required to keep the polymer at a certain extension compared to a lower temperature. For single PNiPAM molecules, as investigated here, we do not observe a sharp transition, which is rather attributed to cooperative effects as discussed in Futscher et al.,²⁷ but a gradual change.

The simulation of isotactic PNiPAM (Figure 6a, open rhombi) shows a similar linear relation of free energy F/L_0 with force. Here, due to the one-sided arrangement of the NiPAM monomer units, hydrogen bond bridges can be formed between two monomers. This presumably leads to a greater influence of the hydrogen bond bridges compared to the syndiotactic polymer, where the NiPAM monomer units are arranged in an alternating fashion with respect to the backbone leading to a less pronounced increase of free energy F/L_0 with force (Figure 6a, filled squares). Additionally, the magnitude of the experimental values for free energy per length F/L_0 (atactic polymer, Figure 6a, solid lines) is close to the simulated syndiotactic data (Figure 6a, open squares) while the simulated

isotactic values (Figure 6a, open diamonds) are about 1.5 times higher for a given force in the range of 200–500 pN. In conclusion, the tacticity of PNiPAM is more important for the free energy to stretch the polymer at a given force than a change of temperature from 278 to 328 K.

CONCLUSION

In a combined experimental and simulation approach, we have scrutinized the temperature dependence of single PEG and PNiPAM polymers. We have been able to develop a reliable procedure to covalently attach long polymers (at least 300 nm) to the tip of a Si₃N₄ AFM cantilever. This allows us to measure highly reproducible single polymer force–extension curves up to high stretching forces (approximately 800 pN), excluding any interactions with neighboring polymer chains, which proved difficult in other experiments (e.g., nanofishing). Our truly single molecule experiments are consistent with MD simulations in explicit solvent at various temperatures. For PNiPAM we could show that neither the shape nor the frequency of the recorded force–extension curves is significantly changed around the LCST at the investigated forces. The LCST is therefore indeed a cooperative effect.

In addition, we find that PEG and PNiPAM show a contrasting temperature stretching response in water. While the stretching force increases with increasing temperature for PNiPAM, a decrease in the stretching force for increasing temperatures can be observed for PEG. The experimental temperature-dependent stretching response of PEG and PNiPAM is also in good agreement with the MD simulation.

Furthermore, both experimental data and MD simulations show a decrease of the force dependent stretching free energy of PEG with increasing temperature for stretching forces starting at about 100 pN. This can be explained by the influence of temperature on the mean fraction of gauche and trans states of the PEG chain and the corresponding reduction of the number of water bridges during stretching. PNiPAM already shows a nonlinear dependence of the free energy per length on temperature at the lowest probed stretching forces (approximately 10 pN).

In summary both single PEG and PNiPAM molecules do not represent purely entropic springs. Their stretching free energy is dominated by energetic solvation effects at a wide range of stretching forces. This shows that although the FJC and WLC models are very helpful for comparing polymer properties, the physical interpretation of the resulting parameters has to be done with care. In particular, as has been found before, both models do not mimic the force–extension behavior over the full range of stretching forces. Here we could further show that they also do not correctly describe the temperature-dependent force–extension behavior, in particular for highly stretched polymers under aqueous conditions.

We propose using the exponent n of the temperature dependence of the normalized stretching free energy (F/L_0) as a measure for the degree of energetic vs entropic character of a polymer. A purely entropic chain is defined by $n = 1$, as obtained in the FJC model with temperature independent Kuhn length. For PEG we find a superenergetic stretching response with $n < 0$. For PNiPAM, we find a mixed stretching response with $0 < n < 1$. Thus, we are able to classify the temperature stretching response of different polymers and to show that PEG has a more dominant energetic character than PNiPAM. At the molecular level, both polymers lose hydrogen

bonds with the surrounding water with rising temperature. At the same time, for PNiPAM, intermolecular hydrogen bonds are formed that compensate for that loss. Thus, PNiPAM shows an antagonistic temperature-dependent force–extension stretching response compared to PEG.

This paves the way for understanding temperature responsive polymers and for designing block copolymer structures for a tailor-made temperature behavior. Materials comprising blocks with antagonistic temperature dependence could be used for switches or actuators^{8,64} analogous to the bimetallic effect. In molecular switches, prestressed building blocks could be used to adjust the force range. In addition, current thermoresponsive materials are often cross-linked polymer hydrogels.⁶⁵ In hydrogels, tensile stress might be concentrated on a small fraction of available chains, which locally leads to a very high tensile stress. In addition, small molecular effects, as observed here, might translate into significant macroscopic effects, e.g., in hierarchical structures,⁶⁶ or the devices might be implemented at significant prestress to increase the temperature response. Finally, some future adaptive force sensors could use a polymeric system that can reach or operate in a highly stretched state.⁶⁷

ASSOCIATED CONTENT

Supporting Information

The Supporting Information is available free of charge on the ACS Publications website at DOI: 10.1021/jacs.9b04383.

Supporting text, Table S1, Figures S1–S11, and references (PDF)

AUTHOR INFORMATION

Corresponding Author

*bizan.balzer@physchem.uni-freiburg.de

ORCID

Richard Schwarzl: 0000-0003-0894-8552

Christian Rüttiger: 0000-0003-0374-7890

Thorsten Hugel: 0000-0003-3292-4569

Markus Gallei: 0000-0002-3740-5197

Bizan N. Balzer: 0000-0001-6886-0857

Notes

The authors declare no competing financial interest.

ACKNOWLEDGMENTS

Funded by the Deutsche Forschungsgemeinschaft (DFG, German Research Foundation) under Germany's Excellence Strategy – EXC-2193/1 – 390951807 (B.N.B. and T.H.) and via Grant SFB 765 (R.R.N.). M.G. and C.R. acknowledge partial support in the frame of the LOEWE Project iNAPO by the Hessen State Ministry of Higher Education, Research and the Arts.

REFERENCES

- (1) Bao, Z.; Feng, Y.; Dodabalapur, A.; Raju, V. R.; Lovinger, A. J. High-Performance Plastic Transistors Fabricated by Printing Techniques. *Chem. Mater.* **1997**, *9*, 1299–1301.
- (2) Bienk, E. J.; Mikkelsen, N. J. Application of advanced surface treatment technologies in the modern plastics moulding industry. *Wear* **1997**, *207*, 6–9.
- (3) Chen, C.-T.; Suslick, K. S. One-dimensional coordination polymers: Applications to material science. *Coord. Chem. Rev.* **1993**, *128*, 293–322.

- (4) Gall, K.; Yakacki, C. M.; Liu, Y.; Shandas, R.; Willett, N.; Anseth, K. S. Thermomechanics of the shape memory effect in polymers for biomedical applications. *J. Biomed. Mater. Res., Part A* **2005**, *73A*, 339–348.
- (5) Keddie, J. L.; Jones, R. A. L.; Cory, R. A. Size-Dependent Depression of the Glass Transition Temperature in Polymer Films. *Europhys. Lett.* **1994**, *27*, 59–64.
- (6) Kuroyanagi, S.; Shimada, N.; Fujii, S.; Furuta, T.; Harada, A.; Sakurai, K.; Maruyama, A. Highly Ordered Polypeptide with UCST Phase Separation Behavior. *J. Am. Chem. Soc.* **2019**, *141*, 1261–1268.
- (7) Magnusson, J. P.; Khan, A.; Pasparakis, G.; Saeed, A. O.; Wang, W.; Alexander, C. Ion-sensitive “isothermal” responsive polymers prepared in water. *J. Am. Chem. Soc.* **2008**, *130*, 10852–10853.
- (8) Wei, M.; Gao, Y.; Li, X.; Serpe, M. J. Stimuli-responsive polymers and their applications. *Polym. Chem.* **2017**, *8*, 127–143.
- (9) Huang, H.; Serpe, M. J. Poly(N-isopropylacrylamide) microgel-based etalons for determining the concentration of ethanol in gasoline. *J. Appl. Polym. Sci.* **2015**, *132*, 24106.
- (10) You, Y.-Z.; Kalebaila, K. K.; Brock, S. L.; Oupický, D. Temperature-Controlled Uptake and Release in PNIPAM-Modified Porous Silica Nanoparticles. *Chem. Mater.* **2008**, *20*, 3354–3359.
- (11) Qian, J.; Wu, F. Thermosensitive PNIPAM semi-hollow spheres for controlled drug release. *J. Mater. Chem. B* **2013**, *1*, 3464–3469.
- (12) Geisler, M.; Xiao, S.; Puchner, E. M.; Gräter, F.; Hugel, T. Controlling the structure of proteins at surfaces. *J. Am. Chem. Soc.* **2010**, *132*, 17277–17281.
- (13) Stetter, F. W. S.; Cwiklik, L.; Jungwirth, P.; Hugel, T. Single lipid extraction: the anchoring strength of cholesterol in liquid-ordered and liquid-disordered phases. *Biophys. J.* **2014**, *107*, 1167–1175.
- (14) Li, I. T. S.; Walker, G. C. Signature of hydrophobic hydration in a single polymer. *Proc. Natl. Acad. Sci. U. S. A.* **2011**, *108*, 16527–16532.
- (15) Kienle, S.; Liese, S.; Schwierz, N.; Netz, R. R.; Hugel, T. The effect of temperature on single-polypeptide adsorption. *ChemPhysChem* **2012**, *13*, 982–989.
- (16) Cui, S.; Pang, X.; Zhang, S.; Yu, Y.; Ma, H.; Zhang, X. Unexpected Temperature-Dependent Single Chain Mechanics of Poly(N-isopropyl-acrylamide) in Water. *Langmuir* **2012**, *28*, 5151–5157.
- (17) Liang, X.; Nakajima, K. Nanofishing of a Single Polymer Chain: Temperature-Induced Coil-Globule Transition of Poly(N-isopropylacrylamide) Chain in Water. *Macromol. Chem. Phys.* **2018**, *219*, 1700394.
- (18) Zhang, W.; Zou, S.; Wang, C.; Zhang, X. Single Polymer Chain Elongation of Poly(N-isopropylacrylamide) and Poly(acrylamide) by Atomic Force Microscopy. *J. Phys. Chem. B* **2000**, *104*, 10258–10264.
- (19) Liese, S.; Gensler, M.; Krysiak, S.; Schwarzl, R.; Achazi, A.; Paulus, B.; Hugel, T.; Rabe, J. P.; Netz, R. R. Hydration Effects Turn a Highly Stretched Polymer from an Entropic into an Energetic Spring. *ACS Nano* **2017**, *11*, 702–712.
- (20) Heskins, M.; Guillet, J. E. Solution Properties of Poly(N-isopropylacrylamide). *J. Macromol. Sci., Chem.* **1968**, *2*, 1441–1455.
- (21) Mao, H.; Li, C.; Zhang, Y.; Bergbreiter, D. E.; Cremer, P. S. Measuring LCSTs by novel temperature gradient methods: evidence for intermolecular interactions in mixed polymer solutions. *J. Am. Chem. Soc.* **2003**, *125*, 2850–2851.
- (22) Deshmukh, S. A.; Sankaranarayanan, S. K. R. S.; Suthar, K.; Mancini, D. C. Role of Solvation Dynamics and Local Ordering of Water in Inducing Conformational Transitions in Poly(N-isopropylacrylamide) Oligomers through the LCST. *J. Phys. Chem. B* **2012**, *116*, 2651–2663.
- (23) Chung, J. E.; Yokoyama, M.; Yamato, M.; Aoyagi, T.; Sakurai, Y.; Okano, T. Thermo-responsive drug delivery from polymeric micelles constructed using block copolymers of poly(N-isopropylacrylamide) and poly(butylmethacrylate). *J. Controlled Release* **1999**, *62*, 115–127.
- (24) Okano, T.; Bae, Y. H.; Jacobs, H.; Kim, S. W. Thermally on-off switching polymers for drug permeation and release. *J. Controlled Release* **1990**, *11*, 255–265.
- (25) Kato, D.; Sohn, W. Y.; Katayama, K. Aggregation-Induced Expansion of Poly(N-isopropyl acrylamide) Solutions Observed Directly by the Transient Grating Imaging Technique. *ACS Omega* **2018**, *3*, 8484–8490.
- (26) Abbott, L. J.; Tucker, A. K.; Stevens, M. J. Single Chain Structure of a Poly(N-isopropylacrylamide) Surfactant in Water. *J. Phys. Chem. B* **2015**, *119*, 3837–3845.
- (27) Futscher, M. H.; Philipp, M.; Müller-Buschbaum, P.; Schulte, A. The Role of Backbone Hydration of Poly(N-isopropyl acrylamide) across the Volume Phase Transition Compared to Its Monomer. *Sci. Rep.* **2017**, *7*, 17012.
- (28) Kutnyanszky, E.; Embrechts, A.; Hempenius, M. A.; Vancso, G. J. Is there a molecular signature of the LCST of single PNIPAM chains as measured by AFM force spectroscopy? *Chem. Phys. Lett.* **2012**, *535*, 126–130.
- (29) Harnoy, A. J.; Rosenbaum, I.; Tirosh, E.; Ebenstein, Y.; Shaharabani, R.; Beck, R.; Amir, R. J. Enzyme-Responsive Amphiphilic PEG-Dendron Hybrids and Their Assembly into Smart Micellar Nanocarriers. *J. Am. Chem. Soc.* **2014**, *136*, 7531–7534.
- (30) Duncan, R. Polymer conjugates as anticancer nanomedicines. *Nat. Rev. Cancer* **2006**, *6*, 688–701.
- (31) Chen, J.; Spear, S. K.; Huddleston, J. G.; Rogers, R. D. Polyethylene glycol and solutions of polyethylene glycol as green reaction media. *Green Chem.* **2005**, *7*, 64–82.
- (32) Brandenberger, C.; Mühlfeld, C.; Ali, Z.; Lenz, A.-G.; Schmid, O.; Parak, W. J.; Gehr, P.; Rothen-Rutishauser, B. Quantitative Evaluation of Cellular Uptake and Trafficking of Plain and Polyethylene Glycol-Coated Gold Nanoparticles. *Small* **2010**, *6*, 1669–1678.
- (33) Kjellander, R.; Florin, E. Water structure and changes in thermal stability of the system poly(ethylene oxide)–water. *J. Chem. Soc., Faraday Trans. 1* **1981**, *77*, 2053–2077.
- (34) Balzer, B. N.; Hugel, T. 2.25 - Single-Molecule Detection and Manipulation. In *Polymer Science: A Comprehensive Reference*; Matyjaszewski, K., Möller, M., Eds.; Elsevier: Amsterdam, 2012; pp 629–645.
- (35) Oesterhelt, F.; Rief, M.; Gaub, H. E. Single molecule force spectroscopy by AFM indicates helical structure of poly(ethylene-glycol) in water. *New J. Phys.* **1999**, *1*, 6.1–6.11.
- (36) Bartell, L. S. On the Effects of Intramolecular van der Waals Forces. *J. Chem. Phys.* **1960**, *32*, 827–831.
- (37) Hess, B.; Kutzner, C.; van der Spoel, D.; Lindahl, E. GROMACS 4: Algorithms for Highly Efficient, Load-Balanced, and Scalable Molecular Simulation. *J. Chem. Theory Comput.* **2008**, *4*, 435–447.
- (38) Bussi, G.; Donadio, D.; Parrinello, M. Canonical sampling through velocity rescaling. *J. Chem. Phys.* **2007**, *126*, 014101.
- (39) Parrinello, M.; Rahman, A. Polymorphic transitions in single crystals: A new molecular dynamics method. *J. Appl. Phys.* **1981**, *52*, 7182–7190.
- (40) Essmann, U.; Perera, L.; Berkowitz, M. L.; Darden, T.; Lee, H.; Pedersen, L. G. A smooth particle mesh Ewald method. *J. Chem. Phys.* **1995**, *103*, 8577–8593.
- (41) Lee, H.; Venable, R. M.; Mackerell, A. D.; Pastor, R. W. Molecular dynamics studies of polyethylene oxide and polyethylene glycol: hydrodynamic radius and shape anisotropy. *Biophys. J.* **2008**, *95*, 1590–1599.
- (42) Berendsen, H. J. C.; Grigera, J. R.; Straatsma, T. P. The missing term in effective pair potentials. *J. Phys. Chem.* **1987**, *91*, 6269–6271.
- (43) Jorgensen, W. L.; Tirado-Rives, J. The OPLS optimized potentials for liquid simulations potential functions for proteins, energy minimizations for crystals of cyclic peptides and crambin. *J. Am. Chem. Soc.* **1988**, *110*, 1657–1666.
- (44) Kanduč, M.; Chudoba, R.; Palczynski, K.; Kim, W. K.; Roa, R.; Dzubiella, J. Selective solute adsorption and partitioning around single PNIPAM chains. *Phys. Chem. Chem. Phys.* **2017**, *19*, S906–S916.

- (45) Palivec, V.; Zadrazil, D.; Heyda, J. All-atom REMD simulation of poly-N-isopropylacrylamide thermodynamics in water: a model with a distinct 2-state behavior. *arXiv* **2018**, arXiv:1806.05592.
- (46) Pirzer, T.; Hugel, T. Atomic force microscopy spring constant determination in viscous liquids. *Rev. Sci. Instrum.* **2009**, *80*, 035110.
- (47) Walder, R.; LeBlanc, M.-A.; van Patten, W. J.; Edwards, D. T.; Greenberg, J. A.; Adhikari, A.; Okoniewski, S. R.; Sullan, R. M. A.; Rabuka, D.; Sousa, M. C.; Perkins, T. T. Rapid Characterization of a Mechanically Labile α -Helical Protein Enabled by Efficient Site-Specific Bioconjugation. *J. Am. Chem. Soc.* **2017**, *139*, 9867–9875.
- (48) Barradas, R. G.; Fletcher, S.; Porter, J. D. The hydrolysis of maleimide in alkaline solution. *Can. J. Chem.* **1976**, *54*, 1400–1404.
- (49) Hutter, J. L.; Bechhoefer, J. Calibration of atomic-force microscope tips. *Rev. Sci. Instrum.* **1993**, *64*, 1868–1873.
- (50) Trathnigg, B. Determination of MWD and chemical composition of polymers by chromatographic techniques. *Prog. Polym. Sci.* **1995**, *20*, 615–650.
- (51) Blass, J.; Albrecht, M.; Wenz, G.; Zang, Y. N.; Bennewitz, R. Single-molecule force spectroscopy of fast reversible bonds. *Phys. Chem. Chem. Phys.* **2017**, *19*, 5239–5245.
- (52) Serr, A.; Netz, R. R. Pulling adsorbed polymers from surfaces with the AFM: stick vs. slip, peeling vs. gliding. *EPL* **2006**, *73*, 292.
- (53) Balzer, B. N.; Gallei, M.; Hauf, M. V.; Stallhofer, M.; Wiegler, L.; Holleitner, A.; Rehahn, M.; Hugel, T. Nanoscale friction mechanisms at solid-liquid interfaces. *Angew. Chem., Int. Ed.* **2013**, *52*, 6541–6544.
- (54) Fava, A.; Iliceto, A.; Camera, E. Kinetics of the Thiol-Disulfide Exchange. *J. Am. Chem. Soc.* **1957**, *79*, 833–838.
- (55) Marchand, P.; Marmet, L. Binomial smoothing filter: A way to avoid some pitfalls of least-squares polynomial smoothing. *Rev. Sci. Instrum.* **1983**, *54*, 1034–1041.
- (56) Li, B.; Wang, X.; Li, Y.; Paananen, A.; Szilvay, G. R.; Qin, M.; Wang, W.; Cao, Y. Single-Molecule Force Spectroscopy Reveals Self-Assembly Enhanced Surface Binding of Hydrophobins. *Chem. - Eur. J.* **2018**, *24*, 9224–9228.
- (57) Idota, N.; Nagase, K.; Tanaka, K.; Okano, T.; Annaka, M. Stereoregulation of Thermoresponsive Polymer Brushes by Surface-Initiated Living Radical Polymerization and the Effect of Tacticity on Surface Wettability. *Langmuir* **2010**, *26*, 17781–17784.
- (58) Smith, S. B.; Finzi, L.; Bustamante, C. Direct Mechanical Measurements of the Elasticity of Single DNA Molecules by Using Magnetic Beads. *Science* **1992**, *258*, 1122–1126.
- (59) Marko, J. F.; Siggia, E. D. Stretching DNA. *Macromolecules* **1995**, *28*, 8759–8770.
- (60) Katsumoto, Y.; Tanaka, T.; Sato, H.; Ozaki, Y. Conformational change of poly(N-isopropylacrylamide) during the coil-globule transition investigated by attenuated total reflection/infrared spectroscopy and density functional theory calculation. *J. Phys. Chem. A* **2002**, *106*, 3429–3435.
- (61) Lin, S. Y.; Chen, K. S.; Liang, R. C. Thermal micro ATR/FT-IR spectroscopic system for quantitative study of the molecular structure of poly(N-isopropylacrylamide) in water. *Polymer* **1999**, *40*, 2619–2624.
- (62) Maeda, Y.; Nakamura, T.; Ikeda, I. Changes in the Hydration States of Poly(N-alkylacrylamide)s during Their Phase Transitions in Water Observed by FTIR Spectroscopy. *Macromolecules* **2001**, *34*, 1391–1399.
- (63) Percot, A.; Zhu, X. X.; Lafleur, M. A simple FTIR spectroscopic method for the determination of the lower critical solution temperature of N-isopropylacrylamide copolymers and related hydrogels. *J. Polym. Sci., Part B: Polym. Phys.* **2000**, *38*, 907–915.
- (64) Chen, J.; Liu, M.; Gong, H.; Huang, Y.; Chen, C. Synthesis and Self-Assembly of Thermoresponsive PEG-b-PNIPAM-b-PCL ABC Triblock Copolymer through the Combination of Atom Transfer Radical Polymerization, Ring-Opening Polymerization, and Click Chemistry. *J. Phys. Chem. B* **2011**, *115*, 14947–14955.
- (65) Es Sayed, J.; Lorthioir, C.; Perrin, P.; Sanson, N. PEGylated NiPAM microgels: synthesis, characterization and colloidal stability. *Soft Matter* **2019**, *15*, 963–972.
- (66) Zhu, B.; Jasinski, N.; Benitez, A.; Noack, M.; Park, D.; Goldmann, A. S.; Barner-Kowollik, C.; Walther, A. Hierarchical Nacre Mimetics with Synergistic Mechanical Properties by Control of Molecular Interactions in Self-Healing Polymers. *Angew. Chem., Int. Ed.* **2015**, *54*, 8653–8657.
- (67) Merindol, R.; Delechiave, G.; Heinen, L.; Catalani, L. H.; Walther, A. Modular Design of Programmable Mechanofluorescent DNA Hydrogels. *Nat. Commun.* **2019**, *10*, 528.
- (68) Hugel, T.; Rief, M.; Seitz, M.; Gaub, H. E.; Netz, R. R. Highly Stretched Single Polymers: Atomic-Force-Microscope Experiments versus Ab-Initio Theory. *Phys. Rev. Lett.* **2005**, *94*, 048301.